Geophysical Research Letters

RESEARCH LETTER
10.1029/2020GL088131

Limited Retreat of the Wilkes Basin Ice Sheet During the Last Interglacial

J. Sutter[1,2], O. Eisen[2,3], M. Werner[2], K. Grosfeld[2], T. Kleiner[1], and H. Fischer[1]

[1]Climate and Environmental Physics, Physics Institute, and Oeschger Centre for Climate Change Research, University of Bern, Bern, Switzerland, [2]Alfred Wegener Institute, Helmholtz-Centre for Polar and Marine Research, Bremerhaven, Germany, [3]Department of Geosciences, University of Bremen, Bremen, Germany

Key Points:
- A marine ice sheet instability in the Wilkes Basin would substantially accelerate ice flow in the Talos Dome region
- The Talos Dome ice core record shows no sign of dynamic thinning during the Last Interglacial
- The Wilkes Basin probably remained relatively stable during the Last Interglacial; thus, the majority of ice loss originated from WAIS

Supporting Information:
- Supporting Information S1

Correspondence to:
J. Sutter,
johannes.sutter@climate.unibe.ch

Citation:
Sutter, J., Eisen, O., Werner, M., Grosfeld, K., Kleiner, T., & Fischer, H. (2020). Limited retreat of the Wilkes Basin ice sheet during the Last Interglacial. *Geophysical Research Letters*, *47*, e2020GL088131. https://doi.org/10.1029/2020GL088131

Received 3 APR 2020
Accepted 18 MAY 2020
Accepted article online 30 MAY 2020

Abstract The response of the East Antarctic Ice Sheet to global warming represents a major source of uncertainty in sea-level projections. Thinning of the East Antarctic George V and Sabrina Coast ice cover is currently taking place, and regional ice-sheet instability episodes might have been triggered in past warm climates. However, the magnitude of ice retreat in the past cannot yet be quantitatively derived from paleo-proxy records alone. We propose that a runaway retreat of the George V coast grounding line and subsequent instability of the Wilkes Basin ice sheet would either leave a clear imprint on the water isotope composition in the Talos Dome region or prohibit a Talos Dome ice-core record from the Last Interglacial altogether. Testing this hypothesis, our ice-sheet model simulations suggest that Wilkes Basin ice-sheet retreat remained relatively limited during the Last Interglacial and provide a constraint on Last Interglacial East Antarctic grounding line stability.

Plain Language Summary The Wilkes Basin ice sheet, located in East Antarctica, harbors enough ice to raise global sea level by several meters. Just like the West Antarctic Ice Sheet, it is vulnerable to ocean warming and is currently losing mass at an accelerated pace. The Last Interglacial ca. 130,000 years ago witnessed global temperatures that are probably surpassed during the next decades and serves as a potential analog for a future warmer planet. We show that during this time, one of the largest marine sectors of the East Antarctic Ice Sheet only contributed relatively little to global sea-level rise. This indicates that keeping global temperatures in check could safeguard at least parts of the Antarctic Ice Sheet from irreversible mass loss.

1. Introduction

The marine-based sectors of the West Antarctic Ice Sheet (WAIS) and East Antarctic Ice Sheet (EAIS) are vulnerable to ocean warming and could be destabilized by processes such as hydrofracturing of ice shelves, ice cliff failure, and elevated basal melting at the grounding line. The large Wilkes and Aurora subglacial basins in East Antarctica (see Figure 1a) hold enough ice to raise global sea level by approximately 12 m (Fretwell et al., 2013). In comparison, the potential sea-level contribution of West Antarctica, in case of a complete marine ice sheet collapse, amounts to ~3–4 m (Bamber et al., 2009). This illustrates that the role of the EAIS for long-term future global sea-level rise needs to be critically assessed.

The large potential contribution to sea-level rise of the EAIS is indicated by reconstructions of sea-level high-stands well beyond 10 m for the mid-Pliocene climate optimum (Dumitru et al., 2019; Grant et al., 2019; Miller et al., 2012), which implies a retreated ice margin of the EAIS during this period (theoretically, the Greenland Ice Sheet and WAIS in concert with land-based glaciers and thermal expansion of the oceans could add ~10 m to global sea level). However, uncertainties of sea-level reconstructions going far back in time can be substantial (Rovere et al., 2014). Specifically, it remains an open question whether contributions from the Wilkes and Aurora Basin were playing a major role in late Quaternary (last 400,000 years) sea-level highstands or whether sea-level rise was mainly driven by West Antarctic Ice Sheet collapse and melt-back of the Greenland Ice Sheet (Dutton et al., 2015) during that time period.

Under current climate conditions, local outlet glaciers along the George V and Sabrina Coast are thinning (Rignot et al., 2019), a process that will likely intensify with the ongoing warming trend. Proxy records suggest increased ice discharge in past climate states warmer than the Holocene such as MIS5e, MIS 11 (Wilson et al., 2018), and the mid-Pliocene warm period (Aitken et al., 2016; Cook et al., 2013; Gulick et al., 2017;

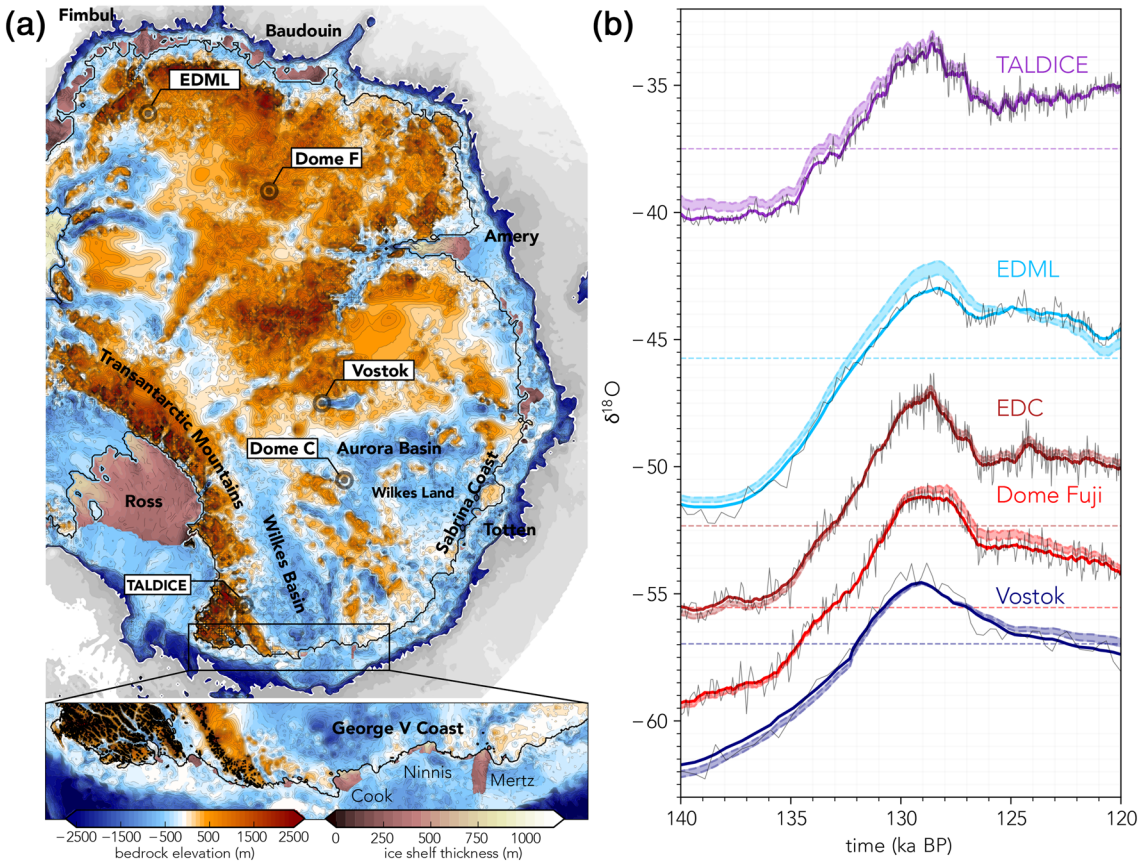

Figure 1. (a) Location of East Antarctic deep ice cores, marine basins, and the present-day grounding line margin (black line, BEDMAP2; Fretwell et al., 2013). The George V Coast and its ice shelves are highlighted in the bottom panel. (b) Ice-core $\delta^{18}O$ records of the East Antarctic ice cores at Talos Dome (TALDICE), EPICA Dronning Maud Land (EDML), EPICA Dome C (EDC), Dome Fuji, and Vostok as temperature proxies covering the Last Interglacial (132–118 ka BP) and Termination II (ca. 140–130 ka BP). Solid colored lines depict data from Masson-Delmotte et al. (2011) (running mean, thin black lines show original data), including the mean Holocene signature (horizontal dashed lines). The shaded curves illustrate the $\delta^{18}O$ record after correction for surface elevation changes in a paleo-ice-sheet simulation (Sutter et al., 2019) using an elevation lapse rate of 0.8 K/100 m (Frezzotti et al., 2007) and a $\delta^{18}O$/temperature gradient of 0.7–1.4 permil/K.

Scherer et al., 2016). Ice sheet modeling studies corroborate these observations, displaying a substantial retreat of the ice margin for both regions forced by a warming of the Southern Ocean beyond approximately 2 K (DeConto & Pollard, 2016; Golledge et al., 2015; Mengel & Levermann, 2014). Ocean warming of this magnitude could be caused by circulation changes, carrying relatively warm circumpolar deep water into ice shelf cavities (Fogwill et al., 2014; Hellmer et al., 2017) and via overall warming of the Southern Ocean due to atmospheric forcing. The CMIP5 model ensemble predicts a regional 21st century warming of Antarctic Shelf Bottom Water of approximately 0.25 K (the water masses relevant for ice shelf melting) even under the strict CO_2 mitigation scenario RCP2.6 (Little & Urban, 2016). Warming might increase toward 2 K in the subsurface of the Pacific sector of the Southern Ocean for scenarios with proliferate greenhouse gas emissions (see Figure S7). This would place end of century ocean warming well within reach of estimated tipping points of both the WAIS and the EAIS (Fischer et al., 2018).

1.1. TALDICE, Recorder of Potential Ice Sheet Instabilities

The underlying hypothesis of this work is that a minor retreat of the George V Coast grounding line could destabilize the Wilkes Basin marine ice sheet (Mengel & Levermann, 2014). We propose that this would lead to a drastic lowering of the ice elevation in the neighboring Talos Dome region leaving an imprint in the water isotope record, which is an archive of paleo-temperatures and sea-ice/ice-sheet changes (Holloway et al., 2016). In fact, the viability of an ice core spanning the last glacial-interglacial cycle at Talos Dome would be questionable for such a scenario as elevated ice flow persisting for millennia would prohibit the

conservation of ice from the Last Interglacial (LIG). The Talos Dome Ice Core (TALDICE) (Frezzotti et al., 2007) drill site is situated on a local ice dome next to the Transantarctic Mountains. The dome rests on the edge of the East Antarctic Plateau close to the South-Pacific sector of the Southern Ocean (see Figure 2). Its location in the headlands of the Wilkes Basin outflow region makes it the ideal recorder of potential episodes of regional grounding line retreat in the past. The TALDICE record continuously covers the LIG and has a maximum age of over 300,000 years (Buiron et al., 2011). Talos Dome is situated relatively close to the major outlet glaciers of the George V Coast (Figure 2) over heavily undulating bedrock in close proximity to deep submarine bedrock troughs. These bedrock troughs protruding hundreds of kilometers into the interior of the East Antarctic Ice Sheet form pathways along which the ice sheet can retreat (Morlighem et al., 2019). One of those bedrock throughs is only a few tens of kilometer west of Talos Dome (see inlet in Figure 2).

In contrast, the continental ice cores EPICA Dome C, Dome Fuji, and Vostok are isolated by much larger distances from the coast, which makes them relatively insensitive to grounding line migration. Their low glacial-interglacial thickness changes (Sutter et al., 2019) and stable water vapor source regions (Masson-Delmotte et al., 2011) make them reliable recorders of large-scale Antarctic climate variations with small elevation change corrections to their isotope-temperature record (see Figure 1b). TALDICE on the contrary might have been influenced by shifts in its isotope source regions and potentially large changes in ice thickness variations. We make use of the relative coherence of the interior ice core records (Dome C, Dome Fuji and Vostok) by investigating surface elevation and ice flow changes at TALDICE in response to a regional instability of the Wilkes Basin ice sheet during the LIG. To estimate the imprint of this instability on the TALDICE δ^{18}O-record, we convert simulated surface elevation changes to temperature assuming a lapse rate of 0.8 K/100 m (Frezzotti et al., 2007) and calculate the changes in local δ^{18}O with a regional isotope/temperature relationship of 0.7–1.4 permil/K derived from Werner et al. (2018).

2. Forcing East Antarctic Ice Sheet Retreat During the LIG

We use the Parallel Ice Sheet Model (PISM Bueler & Brown, 2009; Winkelmann et al., 2011) using 4-, 8-, and 16-km grid resolution employing a subgrid interpolation of the grounding line position and stresses (Feldmann et al., 2014) to allow for a realistic representation of grounding line dynamics at resolutions coarser than 1 km. We do not expect our results to change qualitatively at higher mesh resolution due to the convergence of the ice sheet's response with higher resolution and the fact that the grounding line around the George V coast tends to respond more rapidly at finer grid resolution (see Figure S2). It is important to note that we do not use the subgrid melting option in PISM, which would allow melting underneath partially floating grid nodes, as we think this could overestimate melting slightly and therefore lead to an oversensitive grounding line (Seroussi & Morlighem, 2018). Transient LIG climate forcing is established from Earth System Model snapshot simulations and interpolated in between these snapshots via a climate index, which provides a continuous spatial forcing throughout the LIG (Sutter et al., 2019). The LIG climate snapshot is derived from Pfeiffer and Lohmann (2016). The standalone ice sheet model simulations are initiated from a paleo-spinup at the onset of the LIG (Termination II; 130 ka BP; see Figure S4) and run until the end of the LIG (120 ka BP). We test the null hypothesis (i.e., absence of marine ice sheet instability along the George V Coast) in a control simulation from a transient ensemble run covering the last 2 million years (Sutter et al., 2019). In this control simulation, regional LIG subsurface ocean temperatures are approximately 2 K warmer than present for a short time (between ca. 128.5 and 128.3 kyr BP), but the ice margin remains close to the present-day configuration. Ice elevation changes simulated in the control scenario only lead to a modest imprint on the TALDICE ice core record (see Figure 1b).

To study the effects of a large-scale grounding line retreat on the ice flow at TALDICE, a subshelf melt rate perturbation is applied to the ice shelves of the George V and Sabrina Coast. During this perturbation, we quasi-instantaneously remove ice shelves via enhanced subshelf melting (similar to Martin et al., 2019; S. Sun, personal communication) for a limited amount of time. We switch back to transient LIG conditions at the end of the perturbation period, allowing the ice shelves to regrow. The perturbation is only applied to the ice shelves of the George V and Sabrina Coast while the rest of the ice shelves are forced as in the LIG control simulation.

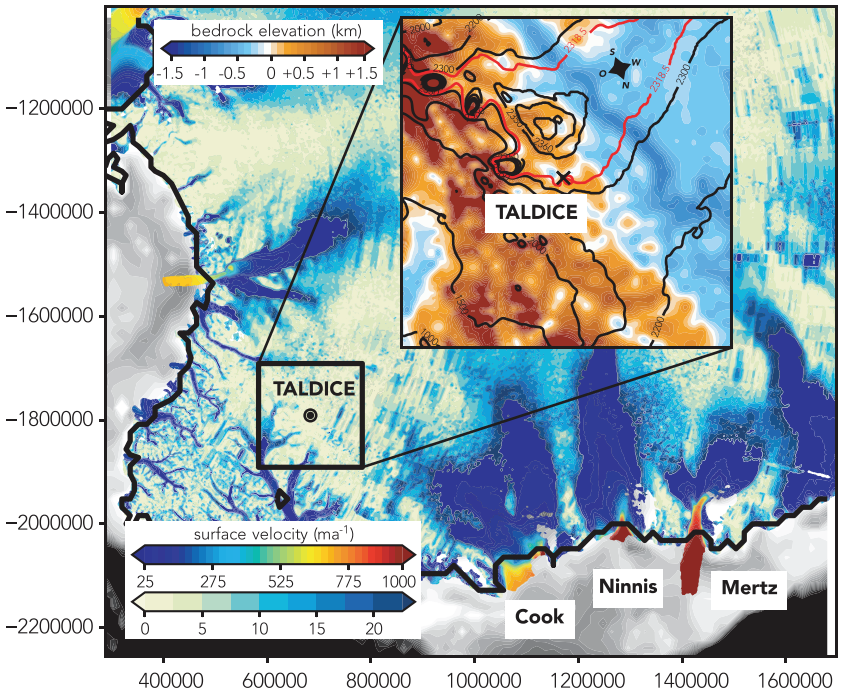

Figure 2. Satellite (InSAR)-derived surface velocities in the study region at 900-m resolution (data from Rignot et al., 2013). The black line depicts the present day grounding line (16-km resolution). The magnified region illustrates the surface contours and bedrock topography around TALDICE (data from Fretwell et al., 2013). Note the deep (≤ −1,000 m) bedrock channel west (grid-right) of TALDICE and the close proximity to the Wilkes Subglacial Basin. Changes in bedrock elevation between BedMachine (Morlighem et al., 2019) and Bedmap2 (Fretwell et al., 2013) can be substantial, potentially affecting simulated ice flow. However, differences in the Talos Dome region are relatively small (Figure S5); therefore, we do not expect our results to be affected significantly.

2.1. Bistable State of the George V Coast Ice Margin During the LIG

The removal of the buttressing force via the prescribed disintegration of the ice shelves leads to a retreat of the ice margin along the George V Coast. We find a tipping point behavior (onset of marine ice sheet instability) upon a certain retreat of the grounding line (see Figure 3), as expected from earlier modeling exercises that use a present day ice sheet configuration (DeConto & Pollard, 2016; Golledge et al., 2019; Mengel & Levermann, 2014; S. Sun, personal communication). Destabilization of the Wilkes Basin is initiated in all experiments by thinning of the Ninnis Glacier (see Videos S1-3) and subsequent retreat along a deep and narrow retrograde (inland-downward) bedrock slope underneath Ninnis Glacier (Morlighem et al., 2019). The Cook Ice stream initially retains constant ice flow due to its advanced frontal position at Termination II but is destabilized ca. 500 years into the simulation for most of the runs due to the propagation of the Ninnis Glacier instability into the Cook Glacier basin (see Movies S1–S5). To trigger irreversible grounding line retreat, the perturbation must be upheld for 300 (4 km), 400 (8 km), and 500 years (16 km) (see Table 1). Higher grid resolution consistently leads to a more sensitive grounding line response most probably due to finer resolution of outlet glaciers and hence faster drainage of ice. Potential pinning points only resolved at higher resolution do not compensate this. The Mertz ice stream is a case in point, as it only retreats in the simulations with 4-km resolution (see Figure S2).

Interestingly, delayed deglaciation of the Wilkes Subglacial Basin occurs in the A-3 experiment (4-km resolution, 300-year perturbation). Removing the ice shelves for 300 years leads to an initial retreat of the Ninnis Glacier front as in the other experiments, while the remaining grounding line is pinned to its initial position at the time of Termination II. After 300 years (the end of the perturbation), ice shelves regrow while high melt rates due to elevated ocean temperatures thin out the ice at the grounding line. Runaway retreat in this scenario is delayed by more than 1,000 years following the same pattern and final extend of grounding line retreat as in the other simulations. It is important to note that the Wilkes Basin ice sheet responds much more sensitively than the Aurora Basin ice cover to the strong perturbation applied here. An advanced ice front largely stabilizes the Sabrina Coastline at the end of Termination II (see Figure S4) in our

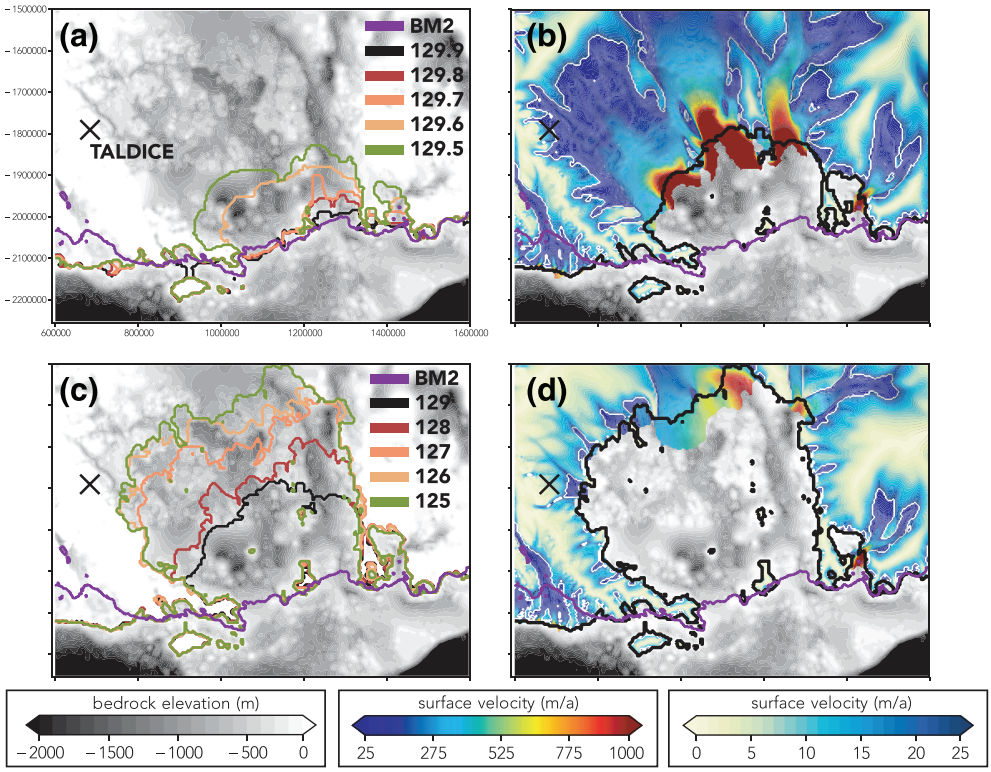

Figure 3. (a) Surface velocity at TALDICE in experiments with 100- (only for 4 km), 300- (dashed lines), and 500-year perturbation time for 4 (red curves), 8 (green curves), and 16 km (blue curves) resolution. (b) Same for TALDICE ice thickness. (c) Same for Wilkes Basin sea-level equivalent ice loss.

experiments and the grounding line remains close to its present day configuration. Recent studies support the notion of relatively stable glaciers along the Sabrina Coast even for strong forcing (Martin et al., 2019; S. Sun, personal communication). We deem our model results to be conservative with regard to grounding line sensitivity as our model setup projects future sea-level contributions on the lower end of the spectrum in model intercomparison studies (Levermann et al., 2019; Seroussi et al., 2019) pointing to a muted dynamic response to external perturbations. Furthermore, the Wilkes Coast ice margin in our model setup is more stable compared to models with ≤1km resolution at the grounding line in perturbation experiments similar to the one applied here but for present-day boundary conditions (S. Sun, personal communication). The main driver of ice sheet retreat in our simulations is clearly the removal of ice shelves along the George V Coast while surface melt is absent as surface temperatures are not warm enough in Pfeiffer and Lohmann (2016). However, Golledge et al. (2017), for example, showed that strong surface warming (≥8K) in this region can lead to surface melt and ice fabric softening in turn driving ice sheet collapse in absence of additional ocean warming.

Table 1
Selected Perturbation Experiments During the Last Interglacial and Corresponding Simulation Names With Corresponding Perturbation Time (Years) and Model Resolution (Res)

P_t (years)	300	400	500
Res 4 km	**A3**	A4	A5
Res 8 km	B3	**B4**	B5
Res 16 km	C3	C4	**C5**

Note. The experiments highlighted in bold depict the minimum time the perturbation has to be upheld to initiate ice sheet collapse (300 a for 4 km, 400 years for 8 km, 500 years for 16 km resolution).

3. Imprint of Wilkes Basin Ice Sheet Collapse on the TALDICE Record

We observe only two stable configurations of the Wilkes Basin ice sheet during the LIG (a persistent feature at all tested resolutions). Either the grounding line retreat is kept in check by the rebounding bedrock and reformation of ice shelves (Talos Dome ice thickness change is limited to 100–200 m), or runaway retreat leads to a 1,000-m near-step-wise decline in ice thickness at Talos Dome (illustrated in Figure 4b). In the stable mode, the expected effect of elevation changes on the isotopic composition in the TALDICE record is moderate and similar to the one simulated in the control simulation. In this case, the sea-level contribution of the Wilkes

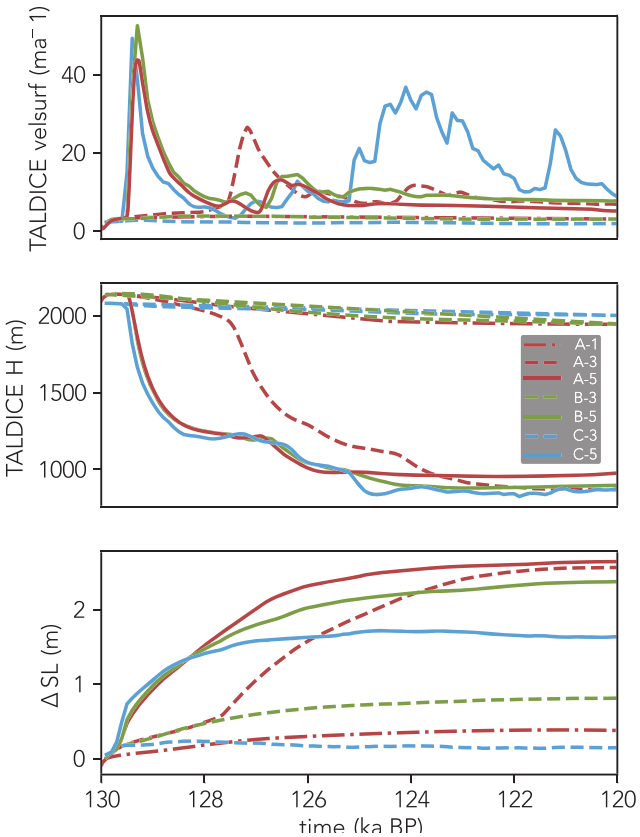

Figure 4. (a,c) Illustration of grounding line retreat at six different time intervalls (legends ka BP) at 4-km resolution and with a 500-year perturbation. BM2 stands for BM2 grounding line (Fretwell et al., 2013). (b) Grounding line position (thick black line) and surface velocity at the time of most rapid surface flow at Talos Dome for same experiment. (d) Same at mid-LIG (125 ka BP). The present-day grounding line derived from Fretwell et al. (2013) is illustrated in rose.

Basin is limited to approximately 0.4–0.8 m (depending on resolution; see Figure 3c). Talos Dome ice thickness is drastically reduced in the unstable mode accompanied by an increase in surface velocity and a sea-level contribution of approximately 1.7–2.5 m (Figure 3c). The drop in surface elevation at Talos Dome would have to be clearly visible as a change of 6–11 permil $\delta^{18}O$ in the isotopic record, yet the observed TALDICE record shows no sudden peak in $\delta^{18}O$ at any time during the LIG. The $\delta^{18}O$ elevation correction at Talos Dome would surpass the interglacial climate signal at TALDICE (~2 permil $\delta^{18}O$ Masson-Delmotte et al., 2011) by a factor of 3–6. However, a reconfiguration of the ice flow around Talos Dome as simulated here would cause a migration of the local ice dome and lead to a steep ice surface gradient across the region (see Figure S6). Therefore, an upstream correction would be required, partly mitigating the elevation correction on the isotope record. To calculate potential upstream corrections, we track the pathways of snowfall in the Talos Dome region during the LIG via passive tracer advection in the ice. It turns out that the steep increase in ice flow (see Figures 3a and 4b) would prohibit a record of LIG atmospheric conditions at Talos Dome altogether as ice from this period would have been already drained into the ocean or frozen to the bed (Movie S5/S6 and Figure S6). We therefore conclude that any retreat of the ice margin in the Wilkes and Aurora subglacial basins during the LIG must have been of limited extent. Consequently, the Antarctic contribution to LIG sea-level rise almost entirely originated from the demise of the West Antarctic Ice or other sectors of the EAIS not discussed here such as the Recovery Glacier (Golledge et al., 2017).

4. Conclusions

The stability of the East Antarctic Ice Sheet in a warming world remains a pressing and as of yet unresolved matter. The outcome emerging from the synthesis of our continental ice sheet modeling exercises with proxy records from ice cores exclude a large-scale retreat of the ice margin of the George V and Sabrina Coast for the LIG. In addition, it provides upper limits for the sea-level contribution of the Wilkes Basin during the LIG of approximately 0.4–0.8 m. Interglacial ice dynamics of marine ice sheets depend not only on the external forcing but also on their preconditioning, for example, through the preceding glacial termination. Therefore, our modeling results for the LIG should not be interpreted as a strict analog for the future behavior of the EAIS. However, our results imply that keeping Antarctic temperatures within LIG levels could warrant the stability of both the George V and Sabrina Coast. This means that strong mitigation efforts as established in the COP21 Paris Agreement, while not necessarily guaranteeing the stability of WAIS, could at least prevent substantial sea-level contributions from the EAIS.

Acknowledgments

We are grateful to the Helmholtz Climate Initiative REKLIM for funding. JS was also supported by the European Union's Horizon 2020 research and innovation program (grant no. 730258 - BE-OI CSA and 820970 - TiPES). HF gratefully acknowledges the long-term support by the Swiss National Science Foundation (SNSF). We thank the Paleoclimate Dynamics group lead by Prof. Gerrit Lohmann for providing climate model output for the Last Interglacial. Computing time was provided by the Alfred-Wegener-Institute.

Data Availability Statement

All data produced in this study are published on Pangaea (https://doi.org/10.1594/PANGAEA.918108) or available from the corresponding author. PISM is available online (https://pism-docs.org/wiki/doku.php). Data sets used in this research are freely available: BEDMAP2 data (Fretwell et al., 2013) is available online (https://secure.antarctica.ac.uk/data/bedmap2/). Last Interglacial climate forcing is available from the corresponding author and described in Pfeiffer and Lohmann (2016).

References

Aitken, A. R. A., Roberts, J. L., van Ommen, T. D., Young, D. A., Golledge, N. R., Greenbaum, J. S., et al. (2016). Repeated large-scale retreat and advance of Totten Glacier indicated by inland bed erosion. *Nature*, *533*(7603), 385–389. https://doi.org/10.1038/nature17447

Bamber, J. L., Riva, R. E. M., Vermeersen, B. L. A., & LeBrocq, A. M. (2009). Reassessment of the potential sea-level rise from a collapse of the West Antarctic Ice Sheet. *Science*, *324*(5929), 901–903. https://doi.org/10.1126/Science.1169335

Bueler, E., & Brown, J. (2009). Shallow shelf approximation as a "sliding law" in a thermomechanically coupled ice sheet model. *Journal of Geophysical Research*, *114*, F03008. https://doi.org/10.1029/2008JF001179

Buiron, D., Chappellaz, J., Stenni, B., Frezzotti, M., Baumgartner, M., Capron, E., et al.(2011). TALDICE-1 age scale of the Talos Dome deep ice core, East Antarctica. *Climate of the Past*, *7*(1), 1–16. https://doi.org/10.5194/cp-7-1-2011

Cook, C. P., van de Flierdt, T., Williams, T., Hemming, S. R., Iwai, M., Kobayashi, M., et al. (2013). Dynamic behaviour of the East Antarctic ice sheet during Pliocene warmth. *Nature Geoscience*, *6*(9), 765–769. https://doi.org/10.1038/Ngeo1889

DeConto, R. M., & Pollard, D. (2016). Contribution of Antarctica to past and future sea-level rise. *Nature*, *531*(7596), 591–597. https://doi.org/10.1038/nature17145

Dumitru, O. A., Austermann, J., Polyak, V. J., Fornos, J. J., Asmerom, Y., Gines, J., et al. (2019). Constraints on global mean sea level during Pliocene warmth. *Nature*, *574*(7777), 233. https://doi.org/10.1038/s41586-019-1543-2

Dutton, A., Carlson, A. E., Long, A. J., Milne, G. A., Clark, P. U., DeConto, R., et al. (2015). Sea-level rise due to polar ice-sheet mass loss during past warm periods. *Science*, *349*(6244), aaa4019. https://doi.org/10.1126/science.aaa4019

Feldmann, J., Albrecht, T., Khroulev, C., Pattyn, F., & Levermann, A. (2014). Resolution-dependent performance of grounding line motion in a shallow model compared with a full-Stokes model according to the MISMIP3d intercomparison. *Journal of Glaciology*, *60*(220), 353–360. https://doi.org/10.3189/2014JoG13J093

Fischer, H., Meissner, K. J., Mix, A. C., Abram, N. J., Austermann, J., Brovkin, V., et al. (2018). Palaeoclimate constraints on the impact of 2° C anthropogenic warming and beyond (vol 11, pg 474, 2018). *Nature Geoscience*, *11*(8), 615–615. https://doi.org/10.1038/s41561-018-0196-3

Fogwill, C. J., Turney, C. S. M., Meissner, K. J., Golledge, N. R., Spence, P., Roberts, J. L., et al. (2014). Testing the sensitivity of the East Antarctic Ice Sheet to Southern Ocean dynamics: Past changes and future implications. *Journal of Quaternary Science*, *29*(1), 91–98. https://doi.org/10.1002/jqs.2683

Fretwell, P., Pritchard, H. D., Vaughan, D. G., Bamber, J. L., Barrand, N. E., Bell, R., et al. (2013). Bedmap2: Improved ice bed, surface and thickness datasets for Antarctica. *Cryosphere*, *7*(1), 375–393. https://doi.org/10.5194/Tc-7-375-2013

Frezzotti, M., Urbini, S., Proposito, M., Scarchilli, C., & Gandolfi, S. (2007). Spatial and temporal variability of surface mass balance near Talos Dome, East Antarctica. *Journal of Geophysical Research*, *112*, F02032. https://doi.org/10.1029/2006JF000638

Golledge, N. R., Keller, E. D., Gomez, N., Naughten, K. A., Bernales, J., Trusel, L. D., & Edwards, T. L. (2019). Global environmental consequences of twenty-first-century ice-sheet melt. *Nature*, *566*(7742), 65–72. https://doi.org/10.1038/s41586-019-0889-9

Golledge, N. R., Kowalewski, D. E., Naish, T. R., Levy, R. H., Fogwill, C. J., & Gasson, E. G. W. (2015). The multi-millennial Antarctic commitment to future sea-level rise. *Nature*, *526*(7573), 421. https://doi.org/10.1038/nature15706

Golledge, N. R., Levy, R. H., McKay, R. M., & Naish, T. R. (2017). East Antarctic ice sheet most vulnerable to Weddell Sea warming. *Geophysical Research Letters*, *44*, 2343–2351. https://doi.org/10.1002/2016gl072422

Grant, G. R., Naish, T. R., Dunbar, G. B., Stocchi, P., Kominz, M. A., Kamp, P. J. J., et al. (2019). The amplitude and origin of sea-level variability during the Pliocene epoch. *Nature*, *574*(7777), 237. https://doi.org/10.1038/s41586-019-1619-z

Gulick, S. P. S., Shevenell, A. E., Montelli, A., Fernandez, R., Smith, C., Warny, S., et al. (2017). Initiation and long-term instability of the East Antarctic Ice Sheet. *Nature*, *552*(7684), 225. https://doi.org/10.1038/nature25026

Hellmer, H. H., Kauker, F., Timmermann, R., & Hattermann, T. (2017). The fate of the southern Weddell Sea continental shelf in a warming climate. *Journal of Climate*, *30*(12), 4337–4350. https://doi.org/10.1175/Jcli-D-16-0420.1

Holloway, M. D., Sime, L. C., Singarayer, J. S., Tindall, J. C., Bunch, P., & Valdes, P. J. (2016). Antarctic last interglacial isotope peak in response to sea ice retreat not ice-sheet collapse. *Nature Communications*, *7*(1), 12293. https://doi.org/10.1038/ncomms12293

Levermann, A., Winkelmann, R., Albrecht, T., Goelzer, H., Golledge, N. R., Greve, R., et al. (2019). Projecting Antarctica's contribution to future sea level rise from basal ice-shelf melt using linear response functions of 16 ice sheet models (LARMIP-2). *Earth System Dynamics Discussions*, *2019*, 1–63. https://doi.org/10.5194/esd-2019-23

Little, C. M., & Urban, N. M. (2016). CMIP5 temperature biases and 21st century warming around the Antarctic coast. *Annals of Glaciology*, *57*(73), 69–78. https://doi.org/10.1017/aog.2016.25

Martin, D. F., Cornford, S. L., & Payne, A. J. (2019). Millennial-scale vulnerability of the Antarctic ice sheet to regional ice shelf collapse. *Geophysical Research Letters*, *46*, 1467–1475. https://doi.org/10.1029/2018gl081229

Masson-Delmotte, V., Buiron, D., Ekaykin, A., Frezzotti, M., Gallee, H., Jouzel, J., et al. (2011). A comparison of the present and last interglacial periods in six Antarctic ice cores. *Climate of the Past*, *7*(2), 397–423. https://doi.org/10.5194/Cp-7-397-2011

Mengel, M., & Levermann, A. (2014). Ice plug prevents irreversible discharge from East Antarctica. *Nature Climate Change*, *4*(6), 451–455. https://doi.org/10.1038/Nclimate2226

Miller, K. G., Wright, J. D., Browning, J. V., Kulpecz, A., Kominz, M., Naish, T. R., et al. (2012). High tide of the warm Pliocene: Implications of global sea level for Antarctic deglaciation. *Geology*, *40*(5), 407–410. https://doi.org/10.1130/G32869.1

Morlighem, M., Rignot, E., Binder, T., Blankenship, D., Drews, R., Eagles, G., et al. (2019). Deep glacial troughs and stabilizing ridges unveiled beneath the margins of the Antarctic ice sheet. *Nature Geoscience*, *13*, 132–137. https://doi.org/10.1038/s41561-019-0510-8

Pfeiffer, M., & Lohmann, G. (2016). Greenland Ice Sheet influence on Last Interglacial climate: Global sensitivity studies performed with an atmosphere-ocean general circulation model. *Climate of the Past*, *12*(6), 1313–1338. https://doi.org/10.5194/cp-12-1313-2016

Rignot, E., Jacobs, S., Mouginot, J., & Scheuchl, B. (2013). Ice-shelf melting around Antarctica. *Science*, *341*(6143), 266–270. https://doi.org/10.1126/science.1235798

Rignot, E., Mouginot, J., Scheuchl, B., van den Broeke, M., van Wessem, M. J., & Morlighem, M. (2019). Four decades of Antarctic Ice Sheet mass balance from 1979-2017. *Proceedings of the National Academy of Sciences of the United States of America*, *116*(4), 1095–1103. https://doi.org/10.1073/pnas.1812883116

Rovere, A., Raymo, M. E., Mitrovica, J. X., Hearty, P. J., O'Leary, M. J., & Inglis, J. D. (2014). The Mid-Pliocene sea-level conundrum: Glacial isostasy, eustasy and dynamic topography. *Earth and Planetary Science Letters*, *387*, 27–33. https://doi.org/10.1016/j.epsl.2013.10.030

Scherer, R. P., DeConto, R. M., Pollard, D., & Alley, R. B. (2016). Windblown Pliocene diatoms and East Antarctic Ice Sheet retreat. *Nature Communications*, *7*, 321–325. https://doi.org/10.1038/ncomms12957

Seroussi, H., & Morlighem, M. (2018). Representation of basal melting at the grounding line in ice flow models. *The Cryosphere*, *12*(10), 3085–3096. https://doi.org/10.5194/tc-12-3085-2018

Seroussi, H., Nowicki, S., Simon, E., Abe-Ouchi, A., Albrecht, T., Brondex, J., et al. (2019). initMIP-Antarctica: An ice sheet model initialization experiment of ISMIP6. *The Cryosphere*, *13*(5), 1441–1471. https://doi.org/10.5194/tc-13-1441-2019

Sutter, J., Fischer, H., Grosfeld, K., Karlsson, N. B., Kleiner, T., Van Liefferinge, B., & Eisen, O. (2019). Modelling the Antarctic Ice Sheet across the mid-Pleistocene transition—Implications for Oldest Ice. *The Cryosphere*, *13*(7), 2023–2041. https://doi.org/10.5194/tc-13-2023-2019

Werner, M., Jouzel, J., Masson-Delmotte, V., & Lohmann, G. (2018). Reconciling glacial Antarctic water stable isotopes with ice sheet topography and the isotopic paleothermometer. *Nature Communications*, *9*, 3537. https://doi.org/10.1038/s41467-018-05430-y

Wilson, D. J., Bertram, R. A., Needham, E. F., van de Flierdt, T., Welsh, K. J., McKay, R. M., et al. (2018). Ice loss from the East Antarctic Ice Sheet during late Pleistocene interglacials. *Nature*, *561*(7723), 383. https://doi.org/10.1038/s41586-018-0501-8

Winkelmann, R., Martin, M. A., Haseloff, M., Albrecht, T., Bueler, E., Khroulev, C., & Levermann, A. (2011). The potsdam parallel ice sheet model (PISM-PIK)—Part 1: Model description. *Cryosphere*, *5*(3), 715–726. https://doi.org/10.5194/Tc-5-715-2011